Cross-regulation of Phosphodiesterase-1 and Phosphodiesterase-2 activities controls dopamine-mediated striatal α-Amino-3-hydroxy-5-methyl-4-isoxazolepropionic Acid (AMPA) Receptor trafficking

Roy S. Song, Rosa Tolentino , Eric A. Sobie, Susana R. Neves-Zaph

Supplementary Materials

Supplementary Text

Model Development We developed a dynamical model of PDE2 regulation of AMPAR trafficking in D1-MSNs. This model was based on our previous model (1), with all the new components/reactions listed in Tables S1 and S2. The novel connectivity is also depicted in Fig. 2A in the main text. The model consists of three-compartments: extracellular space, the plasma membrane, and the cytoplasm. Surface area and volume dimensions for the cytoplasmic compartment are based on ref. (2). AC5 accounts for the majority of the cyclase activity in the striatum (3). We included AC basal activity in the model to account for the rest of the cyclases expressed, and we constrained it based on Fig S2A. We added a basal soluble guanylyl cyclase activity based on ref. (4). We constrained all initial concentrations of ACs, and PDEs with experimental basal and receptor stimulated cAMP values (5). We assumed basal cGMP levels to be 10X less abundant than basal cAMP levels, an assumption based on cGMP and cAMP measurements from other cell types (6), and used this value to constrain PDEs, and sGC initial concentrations.

Initial concentrations are in units of molecules per square micrometer for membrane components and micromolar for cytosolic components (Table S1); for those components not listed on the table, the initial concentrations were set to zero. Components that are never limiting, such as ATP, were labeled as “clamped”. When available, we used kinetic parameter values reported in published experimental studies (Table S2). When kinetic parameters were not available, we used experimental input:output relationships to constrain the model either from published experimental data or from the current study (as shown in Fig S2). All binding reactions were represented using mass action law. Enzymatic reactions were approximated using Michaelis Menten

formalism, except for those involving PDE1 and PDE2. All enzymatic reactions for species of PDE1 or PDE2 were depicted using mass action law as follows:

$$PDE + cNMP \underset{k_r}{\overset{k_f}{\Leftrightarrow}} PDE\_cNMP \overset{k_{cat}}{\rightarrow} PDE + NMP$$

The k_f, k_r and k_{cat} values were calculated from experimental V_{max} and K_m values as follows:
The molecular weight of the enzyme was converted into g/mol. The total amount of enzyme used in the reaction was converted into moles. Vmax was converted into units of mol/sec/mg. k_{cat} was calculated by the equation: Vmax * (1mg/(# of moles of enzyme in reaction)). k_r was calculated by multiplying k_{cat} by 4 (7). k_f was calculated based on $(k_r + k_{cat}) / K_m$.

All experimental inhibitor data (BAY60) were explicitly modeled using second-order reactions involving the drug and its target (Table S2). The full model is available at the Virtual Cell (VCell) web site, http://vcell.org, under "publicly shared models" (username rsong: PDE1_2_Crosstalk_2015). The MATLAB script is available upon request.

Parameter Sensitivity Analysis Parameter sensitivity analysis was performed using a partial least squares (PLS) regression method developed by Sobie (8). The method consists of parameter variation, multiple simulations with the varied parameters, and multivariable regression to determine relationships between parameters and simulation outputs. All initial parameter values were varied randomly one standard deviation of the distribution of the log-transformed initial values. Simulations using the varied parameters were performed, and the resulting timecourse of GluA1 membrane insertion in response to DA was used to calculate the corresponding AUC. The regression analysis calculates a value (regression coefficient, B_{PLS}) that minimizes the difference between the actual value and the computed value given the varied set of parameters. Thus, a low regression coefficient value signifies a parameter that is not sensitive. 1000 trials were conducted to increase the accuracy of the regression analysis. Fig S3A is a scatterplot of actual AUC values of GluA1 membrane insertion computed for each trial of randomized parameter values (x-axis) versus the predicted values (y-axis) performed using the PLS regression. The R^2 value represents the accuracy of the predictions compared to the actual values that is calculated from any given set of parameters. The regression coefficient (B_{PLS}) for each parameter is plotted in Fig S3B. We labeled parameters with B_{PLS} values greater than 0.5 or less than -0.5 as sensitive parameters (8), and listed them in Table S3.

Identified sensitive parameters and randomly selected non-sensitive parameters were further tested in the model, by increasing and decreasing by 25% of their original value and comparing the resulting GluA1 membrane insertion timecourse to experimental data. We plotted the resulting GluA1 membrane insertion timecourse against the experimental timecourse of GluA1 membrane insertion due to D1R stimulation (from Fig S2A). The experimental timecourse is shown with error bars indicating the standard deviation of the mean (Fig S4). Varying sensitive parameter by +/- 25% dramatically alters GluA1 membrane insertion while varying non-sensitive parameter has no effect. In addition, the maximal value of GluA1 membrane insertion from each simulation conducted is plotted against the maximal value from the experimental timecourse (from Fig S2A) with upper and lower bounds representing the standard deviation of the mean for comparison (Fig S5). Increasing or decreasing sensitive parameters result in GluA1 membrane insertion values outside the experimental standard deviation boundaries, while varying non-sensitive parameters has no effect.

Figure S1

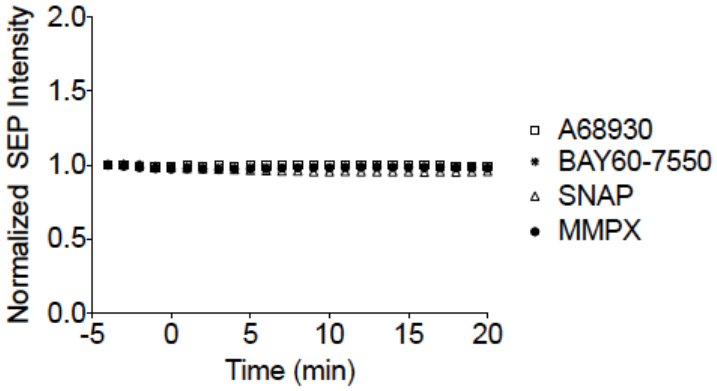

Figure S1 Pharmacological agents used in the current study have no effect on cellular pH
After 5 min baseline, 0.1 µM A68930 (open square; 4 cells), 1.0 µM Bay60-7550 (star; 17 cells), 50 µM SNAP (triangle; 6 cells), or 10 µM MMPX (circle; 7 cells) was added.

Figure S2

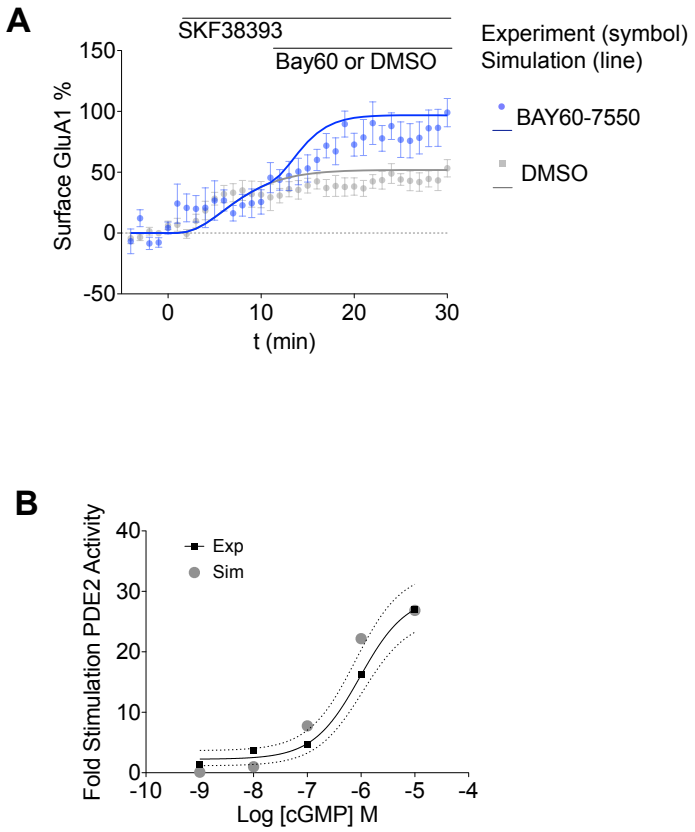

Figure S2 Experimental data used to constrain model

(A) PDE2 inhibition increases GluA1 membrane insertion. A D1R agonist (1.0 μM SKF38393) was added after 5 min baseline, followed by a 1.0 μM BAY60-7550 (blue; 6 cells) or DMSO (gray; 7 cells). Simulation results are shown as blue (Bay60-7550) and black (CT) lines.

(B) cGMP dose response curve of PDE2 activation from experimental data from Surapisitchat et al. (9). Experimental data is shown (average, black squares/line; +/- standard error as dashed lines) and simulation results (gray circles).

Figure S3

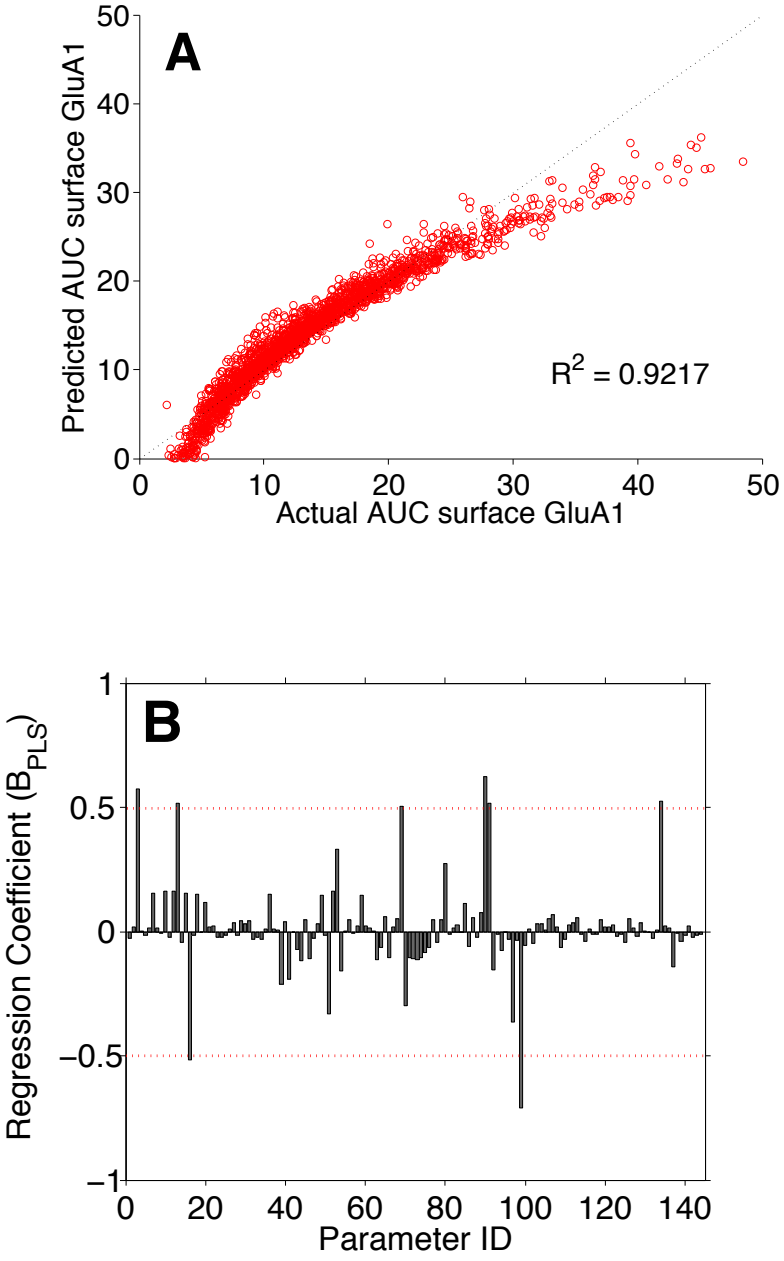

Figure S3 Parameter sensitivity analysis

(A) Actual surface GluA1 AUC values computed from each trial of randomized parameters (x-axis) versus predicted surface GluA1 AUC values (y-axis) from the PLS regression analysis (R^2 value = 0.9217). (B) The regression coefficient generated by the PLS regression analysis (B_{PLS}) for each parameter with red dotted lines indicating the sensitivity threshold.

Figure S4

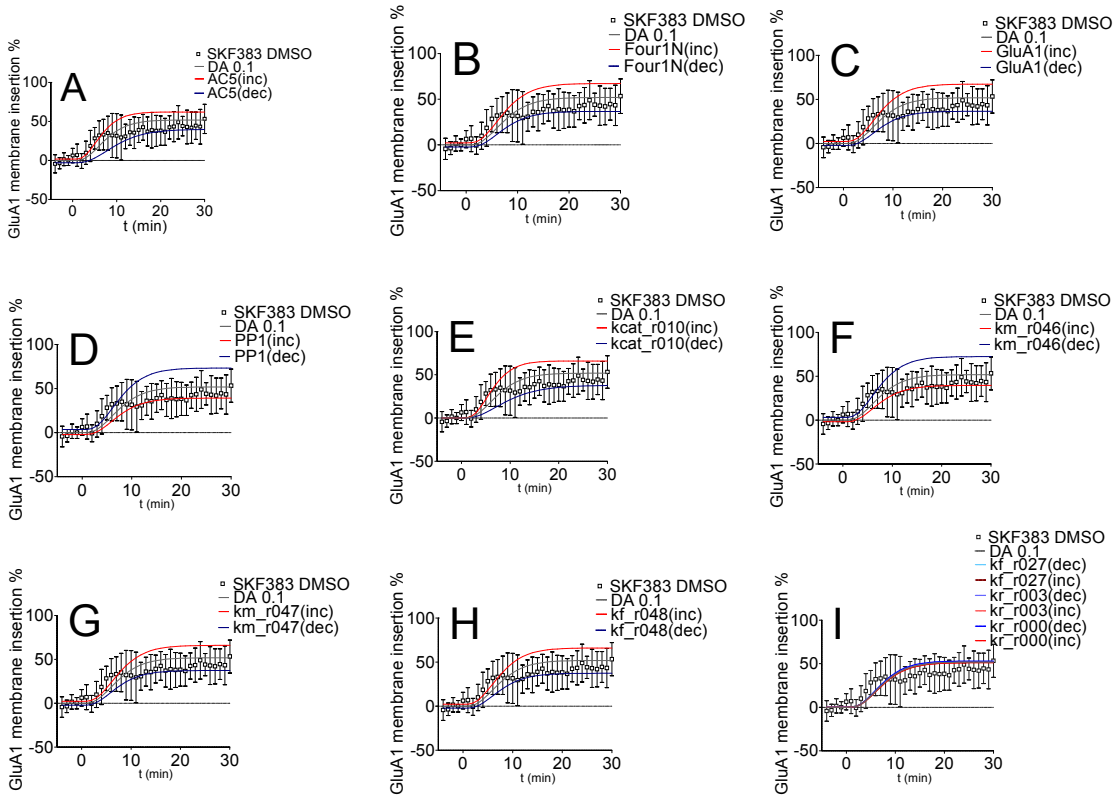

Fig S4 Comparison of identified sensitive and non-sensitive parameters to experimental GluA1 membrane insertion timecourse

Each sensitive parameter (A-H) or non-sensitive parameter (I) was increased (red line) or decreased (blue line) by 25% of its original value. The corresponding simulation of GluA1 membrane insertion timecourse is plotted, versus experimental D1R-stimulated GluA1 membrane insertion timecourse (black square) with error bars indicating the standard deviation of the mean. Gray line represents timecourse simulation with 0.1 μM of DA. A list identifying all parameters is shown in Table S3.

Figure S5

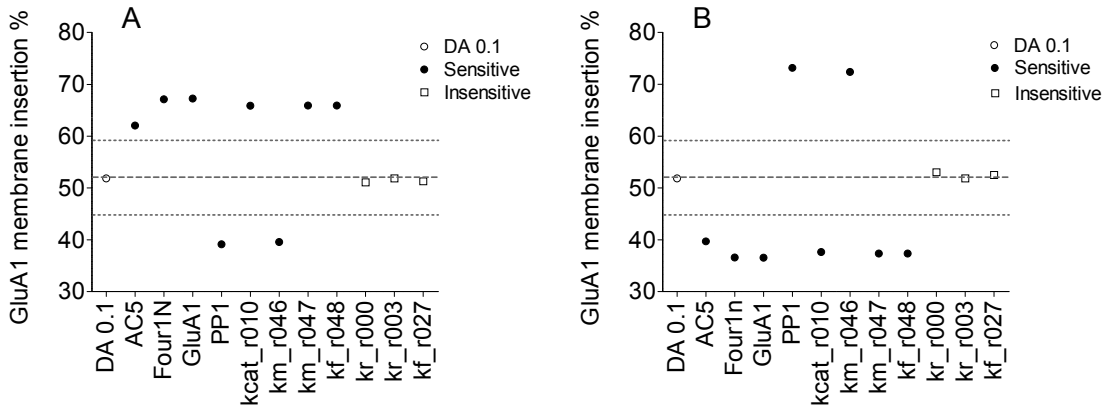

Fig S5 Comparison of identified sensitive and non-sensitive parameters to experimental maximal GluA1 membrane insertion

Maximal GluA1 membrane insertion value from simulations conducted in Fig S4 is plotted. Sensitive (black filled-in circle) parameter and non-sensitive (open square) parameter values were increased by 25% (A) or decreased by 25% (B). The dashed gray line is the mean of last two time points (maximal GluA1 membrane insertion) from experimental D1R-stimulated GluA1 membrane insertion, with dotted lines representing +/- standard deviation. Open circle represent simulation with 0.1 μM of DA.

`

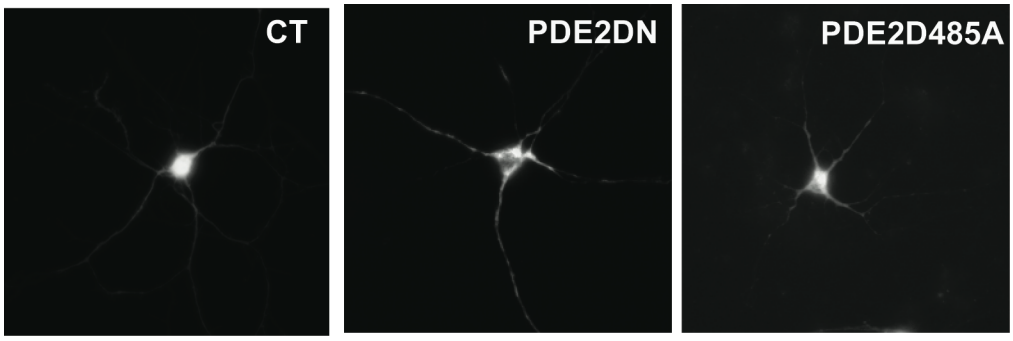

Fig S6 Cellular expression of PDE2 mutants in MSNs
Representative images of the cellular expression of PDE2 mutants PDE2DN and PDE2D485A in MSNs from experiments shown Fig 4.

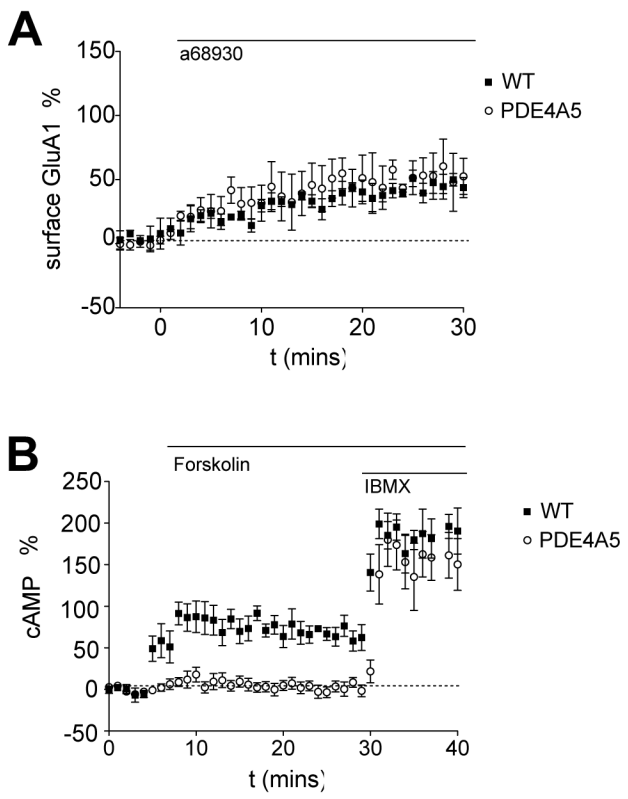

Fig S7 Overexpression of a non-striatal enriched PDE does not affect D1-induced increase in GluA1 surface expression. (A) PDE4A5 overexpression does not affect surface GluA1 levels induced by D1 stimulation in D1-MSNs (open circles; 5 cells). (A) PDE4A5 overexpression significantly decreases cAMP levels induced by 13 μM forskolin in MSNs (open circles: 8 cells; black square: 4 cells).

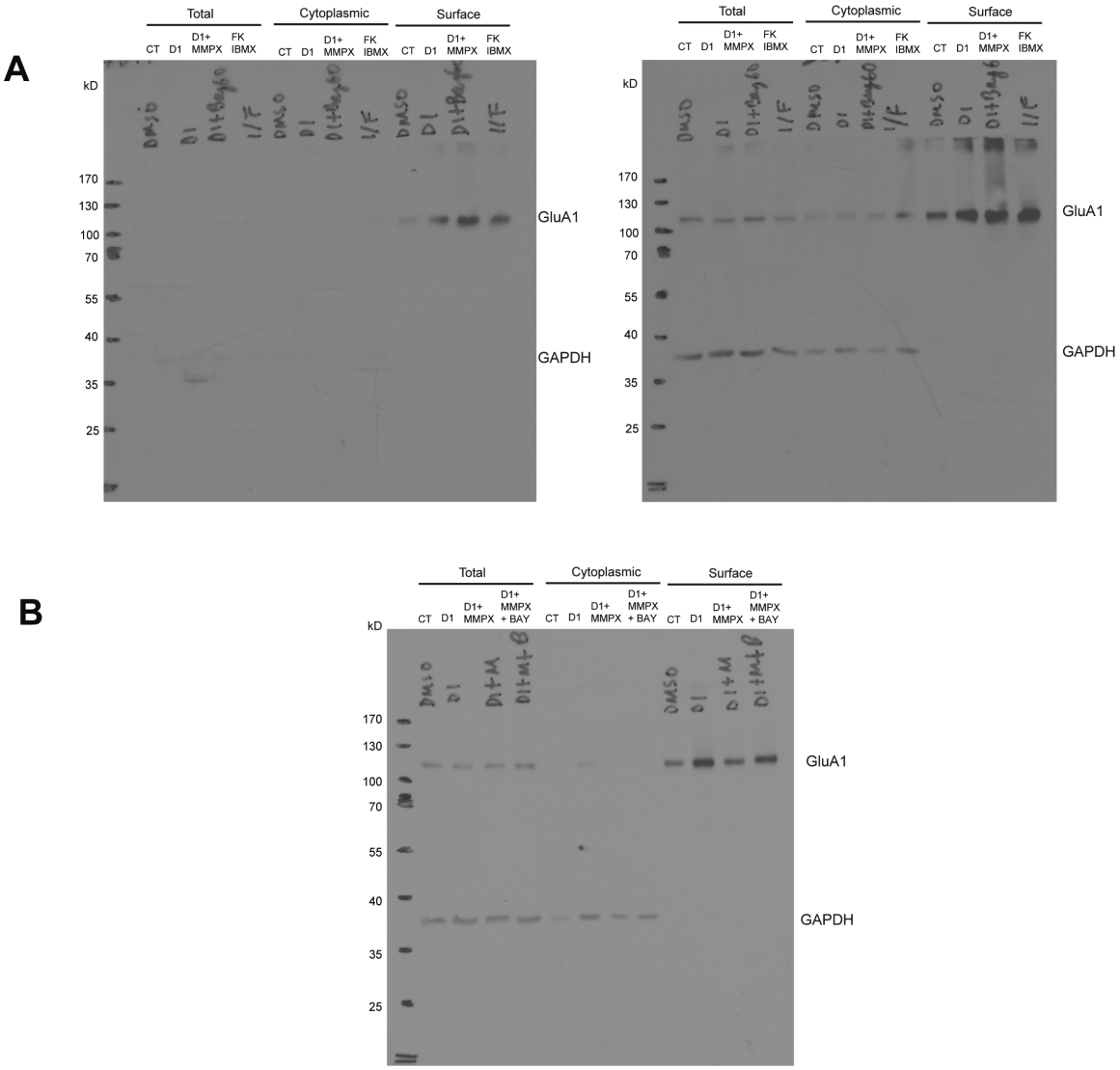

Fig S8 Full images of immunoblots shown in Fig 7. (A) PDE2 inhibition increases D1-induced surface GluA1; (left panel) short exposure to show surface GluA1; (right panel) long exposure to show total GluA1 and GAPDH. (B) PDE1 inhibition decreases D1-induced surface GluA1.

Table S1 Initial Concentrations

Species	Initial concentrations	Units	Reference
sGC	0.15	μM	Estimated
sGC is activated by SNAP treatment.			
sGC_basal	0.15	μM	(6)
sGC_basal was added to maintain a basal cGMP concentration ~0.01 μM, 10 fold lower than cAMP based on (6).			
GTP (clamped)	500	μM	(10)
GTP concentration based on (10).			
PDE1	0.5	μM	Assumed
PDE2	0.5	μM	Assumed
ACbg	15	molecules*μm^{-2}	(5)
Background AC added to maintain basal cAMP concentration ~0.1 μM (5).			
PDEbg_cAMP	0.1	μM	Estimated
Background cAMP PDE was added to ensure that cAMP does not exceed ~1.5 μM when both PDE1 and PDE2 are inhibited, based on cAMP levels induced by IBMX treatment from (5). This accounts for PDEs not represented in the model.			
PDEbg_cGMP	0.1	μM	Estimated
Background cGMP PDE was added to ensure that cGMP does not exceed ~0.15 μM when both PDE1 and PDE2 are inhibited, based on cAMP levels induced by IBMX treatment from (5). This accounts for PDEs not represented in the model.			

Table S2 Reaction parameters

Michaelis-Menten Reactions

Enzyme	**Substrate**	**Product**	**Km (μM)**	**kcat (s^{-1})**	**Reference**
ACbg	ATP	cAMP	1030	0.9	(1,5)
We maintained the Km for ACbg same as Km for basal activity of AC5. kcat for ACbg was increased to maintain a basal cAMP concentration of ~0.1 μM (1,5).					
PDEbg_cAMP	cGMP	AMP	10	25	Estimated
The Km and kcat values for background cAMP PDE were constrained to maintain basal cAMP concentration ~0.1 μM and to ensure that cAMP does not exceed ~1.5 μM when both PDE1 and PDE2 are inhibited, based on cAMP levels induced by IBMX treatment from (6).					
sGC_basal	GTP	cGMP	100	0.18	(4)
Basal sGC rate constants based on (4)					
PDEbg_cGMP	cGMP	GMP	25	25	Estimated
The Km and kcat values for background cGMP PDE were chosen to maintain basal cGMP concentration ~0.01 μM and to ensure that cGMP does not exceed ~0.15 μM to account for PDEs not represented in the model.					
sGC_active	GTP	cGMP	45	7.35	(4,11)
Active sGC rates based on (4,11)					

Mass Action Reactions

Reactions	**kf**	**Units**	**kr**	**Units**	**Reference**
PDE1+cAMP←→ PDE1_cAMP	0.36	s^{-1}* μM^{-1}	18.9	s^{-1}	(12)
PDE1_cAMP←→ PDE1+AMP	4.73	s^{-1}	0	s^{-1}* μM^{-1}	
MW PDE1B = 63kDa; we calculated the rate constants based on basal PDE1 activity Km=66 μM and Vmax=1.76 μmol/min/mg values from (12)					
PDE1+cGMP←→ PDE1_cGMP	7.0	s^{-1}* μM^{-1}	33.6	s^{-1}	(12)
PDE_cGMP←→ PDE1+GMP	8.4	s^{-1}	0	s^{-1}* μM^{-1}	
MW PDE1B = 63kDa; we calculated the rate constants based on Km=6 μM and Vmax=8 μmol/min/mg values from (12).					
PDE2+cAMP←→ PDE2_cAMP	3.5	s^{-1}* μM^{-1}	84	s^{-1}	(13)
PDE2_cAMP←→ AMP+PDE2	21	s^{-1}	0	s^{-1}* μM^{-1}	
MW PDE2A =105kDa; we calculated the rate constants based on Km=30 μM and Vmax=120 μmol/min/mg values from (13). Rate constants were scaled down to fit Fig S2A.					
PDE2+cGMP←→ PDE2_cGMP	10.7	s^{-1}* μM^{-1}	86.0	s^{-1}	(13)
PDE2_cGMP←→ PDE2+cGMP	21.5	s^{-1}	0	s^{-1}* μM^{-1}	
MW PDE2A =105kDa; we calculated the rate constants based on Km=10 μM and Vmax=123 μmol/min/mg values from (13).					
PDE2+cGMP←→ PDE2_active	4.1	s^{-1}* μM^{-1}	0.9	s^{-1}	(9)
Rate constants for activation of PDE2 by cGMP were based on cGMP effect on PDE2 cAMP hydrolytic activity from (9) and Fig S2B.					
PDE2_active+cAMP←→ PDE2_active_cAMP	14	s^{-1}* μM^{-1}	84	s^{-1}	(13,14)
PDE2_active_cAMP←→	84	s^{-1}	0	s^{-1}* μM^{-1}	

PDE2_active+AMP					
cGMP activated PDE2 increases cAMP hydrolytic activity by ~3.5-6 fold (13,14). kf and kcat values for cAMP hydrolysis by active PDE2 were scaled up, assuming a Km of 12 (2.5X lower than basal Km).					
PDE2_active+cGMP←→ PDE2_active_cGMP	10.7	s^{-1}* μM^{-1}	86	s^{-1}	(13)
PDE2_active_cGMP←→ GMP+PDE2_active	21.5	s^{-1}	0	s^{-1}* μM^{-1}	
MW PDE2A =105kDa; Km=10 μM and Vmax=123 μmol/min/mg were used to calculate the rate constants based on (13).					
MMPX + PDE1 ←→ PDE1_inhibited	1.0	s^{-1}* μM^{-1}	1.2	s^{-1}	(15)
Rate constants were constrained using experimental IC_{50} = 5.2 μM (15).					
BAY60 + PDE2 ←→ PDE2_inhibited	1.0	s^{-1}* μM^{-1}	0.01	s^{-1}	(16)
Rate constants were constrained using the IC_{50} = 0.0047 μM (16) and from Fig S2A.					
SNAP + sGC_inactive ← → sGC_active	1.0	s^{-1}* μM^{-1}	0.25	s^{-1}	(11,17)
SNAP is a NO donor. The K_D (0.25 μM) of NO to sGC was used (11,17) to estimate SNAP rate constants.					

Table S3

B_{PLS} Value	**Parameter name**	**Reaction information**
0.52303	AC5	Initial concentration
0.51671	Four1N	Initial concentration
0.62273	GluA1	Initial concentration
-0.7086	PP1	Initial concentration
0.5023	kcat_r010	ATP->cAMP (AC5_Ga)
-0.51502	km_r046	GluA1->GluA1_845 (PKA)
0.5155	km_r047	GluA1_845->GluA1(PP1)
0.57578	kf_r048	Four1N+GluA1_845<->AMPAR

Table S3 Sensitive parameters identified by PLS regression analysis
List of sensitive parameters identified from the PLS regression analysis with their corresponding regression coefficient values (B_{PLS}).

References:

1. Song, R. S., Massenburg, B., Wenderski, W., Jayaraman, V., Thompson, L., and Neves, S. R. (2013) ERK regulation of phosphodiesterase 4 enhances dopamine-stimulated AMPA receptor membrane insertion. *Proceedings of the National Academy of Sciences of the United States of America* **110**, 15437-15442
2. Routh, B. N., Johnston, D., Harris, K., and Chitwood, R. A. (2009) Anatomical and electrophysiological comparison of CA1 pyramidal neurons of the rat and mouse. *Journal of neurophysiology* **102**, 2288-2302
3. Iwamoto, T., Okumura, S., Iwatsubo, K., Kawabe, J., Ohtsu, K., Sakai, I., Hashimoto, Y., Izumitani, A., Sango, K., Ajiki, K., Toya, Y., Umemura, S., Goshima, Y., Arai, N., Vatner, S. F., and Ishikawa, Y. (2003) Motor dysfunction in type 5 adenylyl cyclase-null mice. *The Journal of biological chemistry* **278**, 16936-16940
4. Wolin, M. S., Wood, K. S., and Ignarro, L. J. (1982) Guanylate cyclase from bovine lung. A kinetic analysis of the regulation of the purified soluble enzyme by protoporphyrin IX, heme, and nitrosyl-heme. *The Journal of biological chemistry* **257**, 13312-13320
5. Mironov, S. L., Skorova, E., Taschenberger, G., Hartelt, N., Nikolaev, V. O., Lohse, M. J., and Kugler, S. (2009) Imaging cytoplasmic cAMP in mouse brainstem neurons. *BMC neuroscience* **10**, 29
6. Eigenthaler, M., Nolte, C., Halbrugge, M., and Walter, U. (1992) Concentration and regulation of cyclic nucleotides, cyclic-nucleotide-dependent protein kinases and one of their major substrates in human platelets. Estimating the rate of cAMP-regulated and cGMP-regulated protein phosphorylation in intact cells. *European journal of biochemistry / FEBS* **205**, 471-481
7. Bhalla, U. S., and Iyengar, R. (1999) Emergent properties of networks of biological signaling pathways. *Science* **283**, 381-387
8. Sobie, E. A. (2009) Parameter sensitivity analysis in electrophysiological models using multivariable regression. *Biophysical journal* **96**, 1264-1274
9. Surapisitchat, J., Jeon, K. I., Yan, C., and Beavo, J. A. (2007) Differential regulation of endothelial cell permeability by cGMP via phosphodiesterases 2 and 3. *Circulation research* **101**, 811-818
10. Traut, T. W. (1994) Physiological concentrations of purines and pyrimidines. *Molecular and cellular biochemistry* **140**, 1-22
11. Kuroda, S., Schweighofer, N., and Kawato, M. (2001) Exploration of signal transduction pathways in cerebellar long-term depression by kinetic simulation. *The Journal of neuroscience : the official journal of the Society for Neuroscience* **21**, 5693-5702
12. Sharma, R. K., and Wang, J. H. (1986) Calmodulin and Ca2+-dependent phosphorylation and dephosphorylation of 63-kDa subunit-containing bovine brain calmodulin-stimulated cyclic nucleotide phosphodiesterase isozyme. *The Journal of biological chemistry* **261**, 1322-1328
13. Martins, T. J., Mumby, M. C., and Beavo, J. A. (1982) Purification and characterization of a cyclic GMP-stimulated cyclic nucleotide phosphodiesterase from bovine tissues. *The Journal of biological chemistry* **257**, 1973-1979
14. Sonnenburg, W. K., Mullaney, P. J., and Beavo, J. A. (1991) Molecular cloning of a cyclic GMP-stimulated cyclic nucleotide phosphodiesterase cDNA. Identification and distribution of isozyme variants. *The Journal of biological chemistry* **266**, 17655-17661
15. Wells, J. N., and Miller, J. R. (1988) Methylxanthine inhibitors of phosphodiesterases. *Methods in enzymology* **159**, 489-496
16. Boess, F. G., Hendrix, M., van der Staay, F. J., Erb, C., Schreiber, R., van Staveren, W., de Vente, J., Prickaerts, J., Blokland, A., and Koenig, G. (2004) Inhibition of

phosphodiesterase 2 increases neuronal cGMP, synaptic plasticity and memory performance. *Neuropharmacology* **47**, 1081-1092

17. Stone, J. R., and Marletta, M. A. (1996) Spectral and kinetic studies on the activation of soluble guanylate cyclase by nitric oxide. *Biochemistry* **35**, 1093-1099